

# Enhancing tribological performance of the magnetic tape/guide interface by laser surface texturing

Bart Raeymaekers,<sup>a,\*</sup> Izhak Etsion,<sup>b</sup> and Frank E. Talke<sup>a</sup>

<sup>a</sup>Center for Magnetic Recording Research, University of California San Diego, La Jolla, CA, 92093, USA

<sup>b</sup>Department of Mechanical Engineering, Technion, Haifa, 32000, Israel

Received 19 October 2006; accepted 20 February 2007; published online 4 April 2007

The friction coefficient is an important parameter in designing magnetic tape transports. We have introduced a novel approach to reduce the friction coefficient between guides and magnetic tape by laser surface texturing the cylindrical guides. The surface features enhance the formation of an air bearing and hence reduce the friction coefficient.

**KEY WORDS:** magnetic tape tribology, foil bearing, belt drive friction, laser surface texturing

## 1. Introduction

Air-lubricated foil bearings are used in a variety of applications such as turbomachinery, journal bearings, dentistry equipment, etc. [1–3]. One of the most intricate applications of air-lubricated foil bearings can be found in magnetic tape drives [4], where a magnetic tape moves over a read/write head and tape drive components such as guides (stationary) and rollers (rotating). Friction is an important parameter in designing a tape transport for a commercial high-performance tape drive. The overall friction force between tape and tape drive components determines the torque needed by the motor to drive the tape and affects the wear of the tape. Metal particulate (MP) tape is widely used in commercial tape recording systems since the tribological performance of the magnetically superior metal evaporated (ME) tape is inferior to that of MP tape.

Lateral tape motion (LTM) is defined as the time-dependent motion of the tape perpendicular to the tape transport direction. It is a friction related phenomenon that can cause track misregistration [5]. Although friction between tape and tape drive components was observed to attenuate LTM [6–8], it is well known that tape drives with pressurized air bearing guides instead of rotating guides exhibit significantly lower LTM than tape drives with rotating guides [9]. Elimination of rotating tape drive components suppresses LTM due to run-out of those components. However, pressurized air bearing guides require an external compressor, which is an obstacle for commercialization of this type of tape drive.

Based on the above information, it is therefore desirable to create an efficient self-acting foil bearing between the tape and the guide, thereby eliminating the need for an external compressor, while still benefiting from a low friction air bearing. In a recent study [10], it was observed that for a tape tension of 1 N, a tape speed of at least 8 m/s was needed to achieve full fluid lubrication and hence, a low friction coefficient. This paper explores the possibility of creating an efficient low speed air bearing between a magnetic tape and a cylindrical guide, thereby expanding the speed range of low friction. We use a novel approach to tape guide design by using laser surface texturing (LST) of the guide surface. We have compared the tribological performance of the laser surface textured guide with various non-textured guides, thereby showing the benefits of textured guide surfaces.

## 2. Laser surface texturing

Laser surface texturing is a well-established technique to create micro-dimples on the surface of tribological components. These dimples act as micro-hydrodynamic bearings, thereby creating a local pressure increase between the sliding surfaces. This, in turn, increases the load carrying capacity for such bearings and reduces the friction coefficient for a constant load. The LST technique has been successfully used in a number of applications, as, for instance, in the manufacturing of metal rolling cylinders with well-defined surface roughness [11] or the fabrication of laser bumps in the landing zone of a hard disk drive to facilitate contact start/stop of the magnetic head [12]. It was, however, not until 1996 that LST was used in conventional lubrication situations as a

\*To whom correspondence should be addressed.  
E-mail: bart@talkelab.ucsd.edu

method to reduce friction and optimize lubrication [13]. LST creates spherically shaped dimples on the surface by means of a material ablation process with a pulsed laser [14]. LST has now successfully been applied in reducing friction in various applications such as piston rings, mechanical seals, and hydrodynamic seals [15–17]. The dimples also allow conducting heat from sliding interfaces and trapping of abrasive wear particles [18]. Hydrodynamic gas seals [19] and hard disk drive technology [20] are applications that are most relevant to the application of LST of the tape/guide interface.

No published investigations exist about magnetic tape guide design in general or texturing of magnetic tape drive components in particular. This paper fills this gap and investigates LST of magnetic tape guide surfaces in order to lower the transition speed between boundary lubrication and full fluid lubrication. This, in turn, reduces tape/guide friction and stiction, provides lower tape/guide wear and would potentially allow the use of ME tape by enhancing its tribological performance.

### 3. Experimental set-up

#### 3.1. Apparatus

While in a real application the tape is sliding over a stationary guide, it is more convenient for the purpose of friction measurement to use a stationary tape sample in combination with a rotating guide [10]. This set-up simulates a moving tape on a stationary guide.

The experimental set up, shown in figure 1, consists of a guide mounted on an adjustable speed DC-motor. A tape sample is positioned over the guide surface and is connected to a load cell that measures the tension  $T_1$  at one end, while at the other end it is subjected to a known tension  $T_2$  by a dead weight (see figure 1a). The load cell is mounted on a sled that can slide in a circular groove to allow a variable wrap angle. Figure 1b indicates the forces  $T_1$  and  $T_2$  and the wrap angle  $\theta$ .

The wrap angle was  $90^\circ$  for all experiments with MP tape and  $45^\circ$  for all experiments with ME tape. The rotational speed of the guide in the clockwise direction is adjustable from 0 to 125 Hz, corresponding to a maximum circumferential speed of about 8 m/s for a guide with a radius of 10 mm. The measured force  $T_1$  combined with the known “slack side” tension  $T_2$  and the wrap angle  $\theta$  enable calculation of the average friction coefficient  $f$  from the ratio  $T_1/T_2$  and the classical belt/pulley equation, given e.g. in [21]:

$$\frac{T_1}{T_2} = \exp(f\theta) \quad (1)$$

#### 3.2. Test specimens

Commercially available MP and ME magnetic tapes were used for the tests. MP tape consists of a polymer substrate, coated with a mixture of metal particles and binder material [22]. The magnetic coating of MP tape also contains abrasive particles for recording head cleaning. ME tape is manufactured by evaporating cobalt on a polymeric substrate in a vacuum chamber. In general, a thin layer of carbon is applied on the magnetic film for wear protection.

A commercial tape drive roller, which was adapted to serve as a guide by removing its bearing, serves as reference case. The commercial guide is coated with ZrN (with small percentages of Ni and W to increase the surface hardness). We compared the tribological performance of the commercial guide (reference) with an aluminum guide that was treated with LST. The LST was applied on the guide with a 5 kHz pulsating Nd:YAG laser with a power of 11 kW and pulses of 30 ns duration and 4 mJ each (courtesy of Surface Technologies Ltd.). The LST surface consists of many dimples (see figure 2). Each of them is characterized by its aspect ratio  $h_p/2r_p$ . In figure 2,  $r_p$  denotes the radius

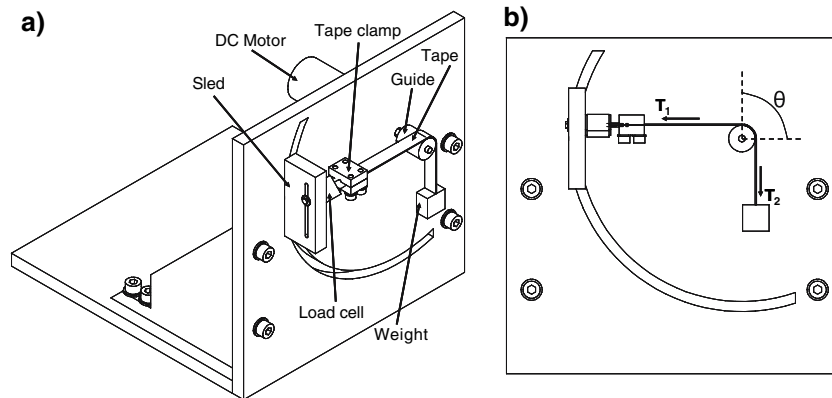


Figure 1. Experimental set-up.

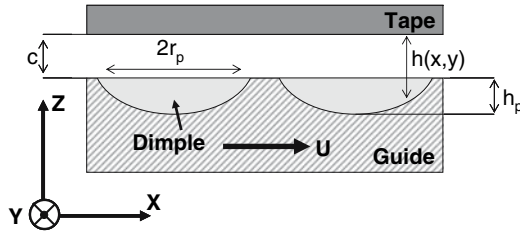


Figure 2. Geometry of the dimples.

of the dimple,  $h_p$  denotes the depth of the dimple,  $c$  is the tape/guide spacing and  $h(x,y)$  is the local spacing between the guide surface and the magnetic tape.  $U$  is the linear speed of the rotating guide. The dimple density  $S_p$  expresses the ratio of the surface covered by dimples versus the total surface area.

The dimples are uniformly distributed over the guide surface. We used an LST guide characterized by the following parameters: (a) a dimple density  $S_p = 0.2$ , (b) a dimple radius  $r_p = 50 \mu\text{m}$ , and (c) a dimple depth  $h_p = 2 \mu\text{m}$ . Figure 3 shows a white light interferometer image (WYKO (Veeco), USA) of a dimpled surface. We also compared the reference case to the case of a ceramic-coated guide and an aluminum-anodized guide. All tested guides had a radius of 10 mm.

Atomic force microscopy (AFM) scans were used for surface roughness measurements of the different guides. The measurements showed that the surface roughness of the guides is isotropic. Hence, the Greenwood–Williamson approach can be used to describe their surface roughness [23].

Table 1 presents the average asperity tip radius  $r$ , the asperity density  $\eta$ , the standard deviation of asperity summit heights  $\sigma_s$ , the ratio  $\sigma_s/r$ , and the dimensionless roughness parameter  $\beta = \eta r \sigma_s$ , for the individual tape samples and guides. The equivalent roughness parameters for two contacting rough surfaces [24] are also shown

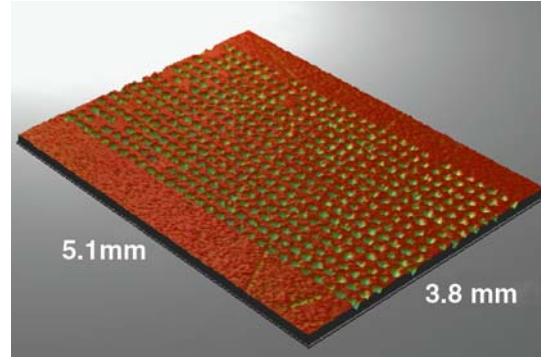


Figure 3. White light interferometer image of dimpled surface.

for eight different tape/guide combinations. These combinations are: (a) ME tape in combination with the commercial tape drive guide (C1), (b) MP tape in combination with the commercial tape drive guide (C2), (c) ME tape in combination with a ceramic guide (C3), (d) MP tape in combination with a ceramic guide (C4), (e) ME tape and an aluminum-anodized guide (C5), (f) MP tape and an aluminum-anodized guide (C6), (g) ME tape and an LST guide (C7), and (h) MP tape and an LST guide (C8).

The values in table 1 were obtained using the three spectral moments  $m_0$ ,  $m_2$ , and  $m_4$  of the surface roughness as described by McCool [24] (see also [10]). The average radius of the asperity tips  $r$ , the asperity density  $\eta$ , and the standard deviation of the asperity summit heights  $\sigma_s$  were calculated and averaged over 15 cross-sections of an AFM scan. From table 1 we observe that the ratio  $\sigma_s/r$  for the commercial guide, the anodized guide, and the LST guide is an order of magnitude smaller than for the ceramic guide, i.e., the surfaces of the commercial guide, the anodized guide, and the LST guide are much smoother than the surface of the ceramic guide. We also observe that the ME tape is much smoother than the MP tape since its  $\sigma_s/r$  value is only one-third of the other material combinations.

Table 1.  
Surface characteristics of the test specimens.

	$r$ (nm)	$\eta$ (nm <sup>-2</sup> )	$\sigma_s$ (nm)	$\sigma_s/r$	$\beta = \eta r \sigma_s$
MP tape	5.55E+03	2.18E-06	5.34	9.62E-04	6.46E-02
ME tape	6.33E+03	2.80E-06	2.10	3.32E-04	3.72E-02
Ceramic	6.36E+02	6.08E-07	376.54	5.92E-01	1.46E-01
LST	1.79E+03	5.91E-07	76.81	4.29E-02	8.13E-02
Commercial	0.90E+03	3.64E-06	20.85	2.31E-02	6.83E-02
Anodized	2.17E+03	5.08E-07	70.72	3.26E-02	7.80E-02
C1	0.85E+03	3.69E-06	21.18	2.49E-02	6.64E-02
C2	0.85E+03	3.65E-06	21.77	2.56E-02	6.77E-02
C3	0.48E+03	7.00E-07	388.02	8.00E-01	1.32E-01
C4	0.48E+03	7.01E-07	388.06	8.01E-01	1.32E-01
C5	2.02E+03	5.44E-07	75.59	3.75E-02	8.29E-02
C6	1.98E+03	5.53E-07	75.77	3.83E-02	8.30E-02
C7	1.70E+03	6.29E-07	77.52	4.56E-02	8.29E-02
C8	1.68E+03	6.36E-07	77.70	4.63E-02	8.30E-02

### 3.3. Test procedure

All tests were carried out at a constant room temperature of 20 °C and a relative humidity of 60%. Tape specimens of 0.1 m length were cut from commercially available tape. For each test a tape sample was connected to the load cell through a tape clamp at one end and a dead weight at the other end, as shown in figure 1a. The MP tape specimens were run-in for 5 min at a rotational speed of  $\omega = 16$  Hz using a tape tension of 0.5 N. Following this run-in procedure, the “slack-side” tension  $T_2$  was adjusted by adding weight, while keeping the DC-motor running, to reach the desired tape tension. The “tight side” tension  $T_1$  was measured for stepwise increments of rotational speeds up to 125 Hz and stored on a PC for further processing. We did not apply the run-in procedure for the ME tape specimens, to avoid damage of the fragile magnetic coating by tape/guide contact. In addition, the “tight side” tension  $T_1$  was measured for stepwise decrements of rotational speeds from 125 Hz down to 16 Hz. Thus, any damage of the coating at the lowest speed does not affect the measurements at higher speeds. These test series were repeated three times for each of the eight combinations C1–C8, with a new tape specimen for each test. The calculated friction coefficient for each test was averaged over its three repetitions.

## 4. Experimental results and discussion

### 4.1. Metal particulate tape

Figure 4 summarizes the results for the experiments with MP tape. These experiments include the commercial guide (C2), ceramic guide (C4), anodized guide (C6), and LST guide (C8), all with a guide radius of 10 mm. We have varied the nominal tape tension between 0.5 and 1.2 N and observed similar behavior in terms of friction coefficient versus tape speed for all cases in that

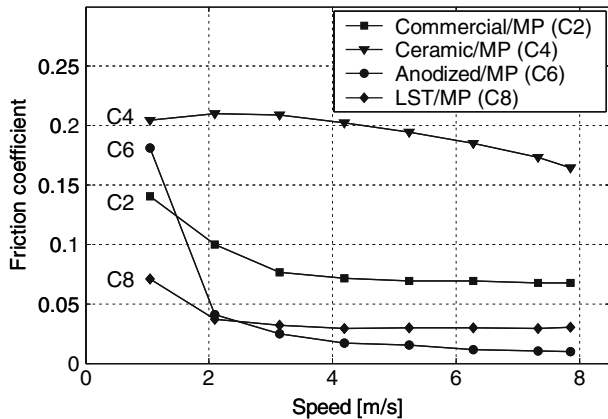


Figure 4. Average friction coefficient versus speed for a tape tension of 1 N, wrap angle of 90° and for a guide radius of 10 mm for combinations C2, C4, C6, and C8.

range. However, we observed that the friction coefficient increased with increasing tape tension, in agreement with the results in [10]. In this paper, we only show results for a tape tension of 1 N, since this is the most commonly used nominal tape tension in state-of-the-art high-performance tape drives. Figure 4 shows the effect of sliding speed on the magnetic tape/guide friction coefficient calculated from equation (1) for a wrap angle,  $\theta$ , of 90°.

From figure 4 we observe that for the case of the commercial guide (C2), the anodized guide (C6), and the LST guide (C8), the friction coefficient asymptotically approaches a very low values of about 0.075 (for the commercial guide), 0.01 (for the anodized guide), and 0.03 (for the LST guide), respectively. These low values are due to the formation of an (partial) air bearing at the tape/guide interface. We note that for the ceramic guide the friction coefficient only decreases from 0.21 at 1 m/s to 0.16 at 8 m/s and hence, never reaches full fluid lubrication in the speed range of our experiments. It is justifiable to assume that full fluid lubrication exists if the tape/guide spacing  $c$  is  $c \geq 3\sigma_s$  [25]. Since the ceramic guide has a much rougher surface than the other guides (see table 1), it is more difficult to obtain full fluid lubrication with this guide (see section 4.3).

The micro-dimples enhance the formation of an air bearing at low speeds and low tape/guide spacing since they increase the average pressure in the air bearing, compared to a non-textured guide surface. At higher speeds when full fluid lubrication has been established and the tape/guide spacing is larger, the influence of the micro-dimples becomes less significant. It is interesting to note that in the full fluid lubrication regime in figure 4, a certain correlation seems to exist between the friction coefficient and the dimensionless roughness parameter  $\beta = \eta r \sigma_s$ , i.e., the friction coefficient decreases as  $\beta$  increases (see figure 4 and table 1).

At a low speed of 1 m/s, the LST guide (C8) has a friction coefficient of 0.07, while the reference commercial guide (C2) has a friction coefficient of 0.14, the anodized guide (C4) has a friction coefficient of 0.18, and the ceramic guide (C6) has a friction coefficient of 0.21. Thus, at low speeds (boundary lubrication) the LST guide outperforms all other guides and has the lowest friction coefficient.

### 4.2. Metal evaporated tape

In order to increase the recording density, tape manufacturers have introduced ME tape, where a high coercivity cobalt film is evaporated and deposited on the tape polymeric substrate in a vacuum chamber. The tribological performance and reliability of ME tape is inferior compared to MP tape [26–28]. Wear protective coatings such as diamond like carbon or a so-called super protective layer have been used to improve the



wear characteristics of ME tape [29]. Osaki [30] pointed out that the magnetic layer of ME tapes is peeled off by increased friction force due to adhesive wear and the relative motion between the tape and the tape drive components. He emphasized the necessity of reducing the friction coefficient between ME tape and tape drive components to increase durability and reliability.

All of the four different guides of our test set-up stalled due to high stiction when attempting to test the ME tape over the full speed range with a guide radius of 10 mm, a wrap angle of  $90^\circ$  and a tape tension of 1 N, i.e., parameters which were previously used with MP tape. Under these conditions the ME tape showed a tendency to “stick” to the guide. To get a complete comparison of the tribological performance for the different guides with the ME tape, we decreased the tape tension to 0.7 N and lowered the wrap angle to  $45^\circ$  to reduce the friction force [10]. Figure 5 presents the results for the experiments with ME tape. These experiments include the commercial guide (C1), the ceramic guide (C3), the anodized guide (C5), and the LST guide (C7), all with a guide radius of 10 mm, a wrap angle of  $45^\circ$  and a tape tension of 0.7 N.

We observe from figure 5 that the ceramic guide (C3) has a high friction coefficient, which is highly dependent on the speed. At 1 m/s the friction coefficient for this guide is almost 0.23, while at 8 m/s it is about 0.05, due to the formation of an (partial) air bearing. The friction coefficient of the commercial guide (C1) approaches 0.05 at 2 m/s and is about 0.13 at 1 m/s. The LST (C7) and anodized (C5) guides are similar at speeds higher than 3 m/s, with a friction coefficient approaching 0.01 (note in table 1 the very similar  $\beta$  values for these two combinations). At 1 m/s, the friction coefficient is about 0.07 for the LST guide and 0.16 for the anodized guide. Again, except for the ceramic guide, all guides reach full fluid lubrication just above 2 m/s (see section 4.3).

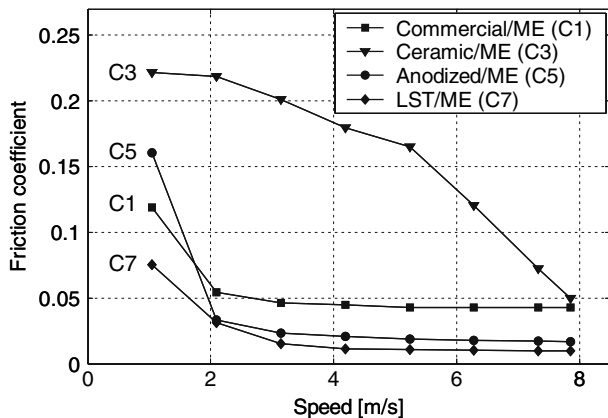


Figure 5. Average friction coefficient versus speed for ME tape with a tape tension of 0.7 N, wrap angle of  $45^\circ$  and a guide radius of 10 mm for the combinations C1, C3, C5, and C7.

Figure 5 (guides with ME tape) and figure 4 (guides with MP tape) reveal the same trend. The ceramic guide has the highest friction coefficient and its friction coefficient is highly dependent on speed. The commercial guide has a slightly higher friction coefficient in the full fluid lubrication regime than the anodized and the LST guides, which may again be explained by lower roughness parameter  $\beta$  of the commercial guide with respect to the anodized and LST guides (see table 1). In the boundary lubrication regime, the LST guide yields a remarkably low friction coefficient because of its dimpled surface and increased air bearing pressure. This very promising result indicates that the use of ME tape in high-performance commercial tape drives could possibly be facilitated with the use of LST guides in the tape path.

The friction coefficient of the LST guide depends less on speed than any of the other tested guides. This is true for both ME and MP tapes. This phenomenon is highly desirable in commercial tape drives since the interaction of the magnetic tape with other tape drive components does not change while the drive is ramping up to operational speed or ramping down to standstill. Hence, the number of start/stop cycles would not affect the wear of the tape, since the friction coefficient is independent of the speed. It should be noted, however, that a direct comparison between figures 4 and 5 must be made with care since the experiments in figure 5 were conducted under modified conditions ( $45^\circ$  wrap angle and 0.7 N tape tension), i.e., stiction effects were eliminated by reducing the friction force between tape and guide.

#### 4.3. Tape/guide spacing

In the literature, simple curve-fit formulas are available that neglect bending stiffness to predict the tape/guide spacing [31]. In our work, we have used the more involved approach discussed in [32] (see also [10]), which includes bending stiffness in the calculation of the tape/guide spacing. We have found that for a smooth guide of radius 10 mm, a tape tension of 1 N and a wrap angle of  $90^\circ$ , the tape/guide spacing yields  $0.163 \mu\text{m}$  at a tape speed of 1 m/s,  $0.2 \mu\text{m}$  at 2 m/s, and  $0.55 \mu\text{m}$  at 8 m/s. Hence, it is clear that full fluid lubrication cannot be established for the ceramic guide at speeds below 8 m/s, since  $c < 3\sigma_s$  for this guide (see table 1). All other guide/tape combinations will reach full fluid lubrication at a speed slightly above 2 m/s. For the case of a smooth guide of radius 10 mm, a tape tension of 0.7 N and a wrap angle of  $45^\circ$ , the tape/guide spacing yields  $0.15 \mu\text{m}$  at a tape speed of 2 m/s and  $0.53 \mu\text{m}$  at a tape speed of 8 m/s. Hence, full fluid lubrication cannot be established for the ceramic guide at speeds below 8 m/s, since again  $c < 3\sigma_s$  for this guide. All other guide/tape combinations will reach full fluid lubrication at a speed just above 2 m/s.

To emphasize the benefit of LST guides at the lowest speed, we have normalized the friction coefficient at a speed of 1 m/s with respect to the relevant commercial guide reference case. In particular, we have used C1 for ME tapes and C2 for MP tapes. Figure 6 shows the normalized average friction coefficient for the eight tape/guide combinations C1–C8.

It was pointed out earlier that the ME and MP experiments are not directly comparable due to their different test parameters. However, we observe clearly that the combinations of LST guide and ME and MP tape, C7 and C8, respectively, yield the lowest friction coefficient of all combinations at a speed of 1 m/s. Compared to the reference case C1, the LST case C7 lowers the friction coefficient by 40%. Compared to the reference case C2, the LST case C8 provides a 50% lower friction coefficient. The anodized and ceramic guides yield higher friction coefficients than their respective reference case at 1 m/s for both ME and MP tapes.

#### 4.4. Friction coefficient model

For tape operating under full fluid lubrication condition, no asperity contact occurs. Hence the friction between guide and tape is entirely due to the viscosity in the air bearing. Since we do not include slip boundary conditions, the average shear stress  $\tau$  in the air bearing can be approximated as

$$\tau_{\text{avg}} = \frac{\mu U}{c} \quad (2)$$

where  $\mu$  is the dynamic viscosity of air,  $U$  the tape speed (see figure 2) and  $c$  is the tape/guide spacing, which is a function of the tape speed. For an LST guide, an equivalent tape/guide spacing  $c_{\text{eq}}$  should be used in equation (2), which incorporates the effect of the dimples. This equivalent clearance depends on an equivalent dimple depth  $h_{\text{eq}}$ , that can be obtained by dividing the

volume of a dimple by the surface of the area of its imaginary square cell [33]:

$$h_{\text{eq}} = \frac{h_p S_p}{6r_p^2} (h_p^2 + 3r_p^2) \quad (3)$$

Hence, the equivalent tape/guide spacing  $c_{\text{eq}}$  can be expressed as

$$c_{\text{eq}} = c + h_{\text{eq}} \quad (4)$$

The friction coefficient  $f$  due to hydrodynamic lubrication can be expressed as

$$f = \frac{\tau_{\text{avg}}}{p_{\text{avg}} - p_a} = \frac{\mu U}{(p_{\text{avg}} - p_a)c_{\text{eq}}} \quad (5)$$

where  $p_{\text{avg}}$  is the average pressure in the air bearing and  $p_a$  is the atmospheric pressure. For untextured (smooth) guides  $h_{\text{eq}} = 0$  and thus  $c_{\text{eq}} = c$ .

Since both the equivalent spacing  $c_{\text{eq}}$  and the average pressure  $p_{\text{avg}}$  are expected to be higher for the LST guides than for the untextured guides, the friction coefficient according to equation (5) will be lower in the full fluid lubrication regime for a textured guide than for a smooth guide. Also, the speed that marks the transition between boundary lubrication and full fluid lubrication regime will be lower in the case of an LST guide. Indeed, if the values of  $p_{\text{avg}}$  and  $c_{\text{eq}}$  are higher for LST guides, the speed  $U$  to obtain a certain friction coefficient  $f$ , that is associated with the transition from boundary lubrication to full fluid film lubrication, will be lower.

In the following we provide a numerical example to validate the theoretical friction calculation. From [34], we know that

$$p_{\text{avg}} - p_a = T/R, \quad (6)$$

where  $T$  is the tape tension per unit tape width and  $R$  is the radius of the tape guide. Thus, combining (5) and (6), one finds

$$f = \frac{\mu UR}{Tc_{\text{eq}}} \quad (7)$$

For a dimple density  $S_p = 0.2$ , dimple depth  $h_p = 2 \mu\text{m}$ , dimple radius  $r_p = 50 \mu\text{m}$ , we calculate from equation (3)  $h_{\text{eq}} = 0.6 \mu\text{m}$ . The transition between boundary lubrication and hydrodynamic lubrication occurs when the minimum tape/guide spacing  $c = 3\sigma_s$  [25]. Hence, for the combination C8 (MP tape and LST guide), we find in table 1 that the transition should occur at  $c = 0.230 \mu\text{m}$ . Thus, by equation (4) we find  $c_{\text{eq}} = 0.83 \mu\text{m}$ . From figure 4 we observe that the

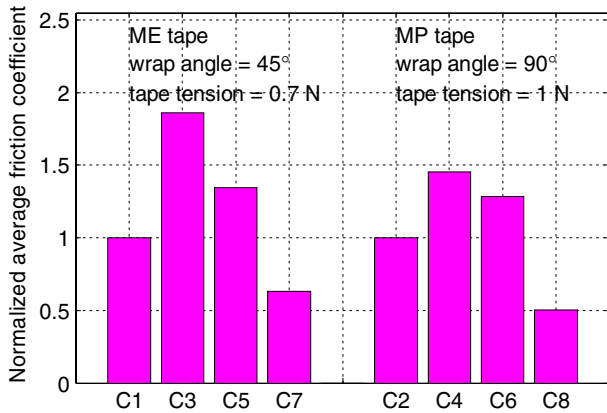


Figure 6. Normalized average friction coefficient for ME and MP tapes with the different guides at a speed of 1 m/s.

transition from boundary lubrication to hydrodynamic lubrication for the combination C8 occurs at  $U = 3$  m/s. For a guide with radius  $R = 10$  mm,  $T = 77$  N/m ( $= 1$  N tension for a 12.7 mm (0.5 in.) wide tape), and  $\mu = 1.81 \times 10^{-5}$ , one finds a friction coefficient of about  $f = 0.01$ , which is on the same order of magnitude of the experimental observation in figure 4.

## 5. Conclusion

1. Laser Surface Textured (LST) guides reduce the friction coefficient between tape and guide, compared to tested commercial and ceramic guides.
2. LST reduces the influence of speed on the friction coefficient. The critical speed where boundary lubrication regime changes into full fluid lubrication decreases significantly for LST guides.
3. ME tape was used successfully in combination with an LST guide at a nominal tape tension of 0.7 N, and wrap angle of  $45^\circ$  even at a tape speed as low as 1 m/s. At this low speed the ME tape tends to “stick” to all other guides (anodized, commercial, and ceramic).

## Acknowledgments

The authors would like to thank Mr. Paul Poorman from Hewlett-Packard for providing commercial tape drive rollers and Mr. Chris Smith from Sony for providing metal evaporated tape. The authors also would like to express their gratitude to Christian Deck and Professor Kenneth Vecchio from the Mechanical and Aerospace Engineering Department at the University of California, San Diego, for providing help with determining the atomic composition of the coating of the commercial roller by means of energy-dispersive X-ray spectroscopy (EDS) analysis. The help of Surface Technologies Ltd. ([www.surface-tech.com](http://www.surface-tech.com)) in providing LST is greatly acknowledged.

## References

- [1] Z.C. Peng and M.M. Khonsari, *J. Trib. T. ASME* 126 (2004) 542.
- [2] Z.C. Peng and M.M. Khonsari, *J. Trib. T. ASME* 126 (2004) 817.
- [3] S. Fields, *Tribol. Lubr. Technol.* 60(4)(2004) 9.
- [4] E. Baugh and F.E. Talke, *Tribol. T.* 39(2)(1996) 306.
- [5] D.B. Richards and M.P. Sharrock, *IEEE T. Mag.* 34(4)(1998) 1878.
- [6] R.J. Taylor and F.E. Talke, *Tribol. Int.* 38 (2005) 599.
- [7] B. Raeymaekers and F.E. Talke, *J. Appl. Mech. T. ASME* (in press) (2007).
- [8] K. Ono, *J. Appl. Mech. T. ASME* 46 (1979) 905.
- [9] R.J. Taylor, P. Strahle, J. Stahl and F.E. Talke, *J. Info. Storage Proc. Syst.* 2 (2000) 255.
- [10] B. Raeymaekers, I. Etsion and F.E. Talke, *Tribol. Lett.* 25(2)(2007) 161.
- [11] J. Crahay and A. Bragard, *Revue de Métallurgie CIT* (1983) 393.
- [12] R. Ranjan, D.N. Lambeth, M. Tromel and Y. Li, *J. Appl. Phys.* 69(8)(1991) 5745.
- [13] I. Etsion and L. Burstein, *Tribol. T.* 39(3)(1996) 667.
- [14] D.A. Scott, M. Brandt, B. Dorien-Brown, B. Valentine P. De, *Opt. Laser Eng.* 18 (1993) 1.
- [15] I. Etsion, *Tribol. Lett.* 17(4)(2004) 733.
- [16] I. Etsion, *J. Trib. T. ASME* 127 (2005) 248.
- [17] G. Duffet, P. Sallamand and A.B. Vannes, *Appl. Surf. Sci.* 205 (2003) 289.
- [18] A. Erdemir, *Tribol. Int.* 38 (2005) 249.
- [19] Y. Kligerman and I. Etsion, *Tribol. T.* 44(3)(2001) 472.
- [20] A.H. Tan and S.W. Cheng, *Tribol. Int.* 39 (2006) 506.
- [21] J.E. Shigley and C.R. Mischke, *Mechanical Engineering Design* 5th ed. (McGraw Hill, New York, 1989).
- [22] M.P. Sharrock, *IEEE T. Mag.* 25(6)(1989) 4374.
- [23] J.A. Greenwood and J.B.P. Williamson, *Proc. R. Soc. Lond. Ser. A Math. Phys. Sci.* 295 (1442) (1966) 300.
- [24] J.I. McCool, *J. Trib. T. ASME* 109 (1987) 264.
- [25] N. Patir and H.S. Cheng, *J. Lubr. Technol. T. ASME* 100(1)(1978) 12.
- [26] M.S. Hempstock and J.L. Sullivan, *IEEE T. Mag.* 32(5)(1996) 3723.
- [27] M.S. Hempstock and J.L. Sullivan, *J. Mag. Mat.* 155 (1996) 323.
- [28] S.T. Patton and B. Bhushan, *Wear* 224 (1999) 126.
- [29] M.D. Bijker, E.A. Draaisma, M. Eisenberg, J. Jansen, N. Persat and E. Sourty, *Tribol. Int.* 33 (2000) 383.
- [30] H. Osaki, *Tribol. Int.* 36 (2003) 349.
- [31] H. Hashimoto and M. Okajima, *J. Trib. T. ASME* 128 (2006) 267.
- [32] C. Lacey and F.E. Talke, *IEEE T. Mag.* 26(6)(1990) 3039.
- [33] Y. Feldman, Y. Kligerman and I. Etsion, *Tribol. Lett.* 22(1)(2006) 21.
- [34] A. Eshel and H.G. Elrod, *J. Basic Eng. T. ASME* 87 (1965) 831.